Chemical Engineering Journal 145 (2009) 505–513

Contents lists available at ScienceDirect

Chemical Engineering Journal

journal homepage: www.elsevier.com/locate/cej

Exploring the regime map for high-shear mixer granulation

Wei-Da Tu [a], Andy Ingram [b], Jonathan Seville [c], Shu-San Hsiau [a,*]

[a] Department of Mechanical Engineering, National Central University, Taiwan 32001, R.O.C
[b] Centre for Formulation Engineering, Department of Chemical Engineering, University of Birmingham, Birmingham B15 2TT, UK
[c] School of Engineering, University of Warwick, Coventry CV4 7AL, UK

ARTICLE INFO

Article history:
Received 21 March 2008
Received in revised form
11 September 2008
Accepted 23 September 2008

Keywords:
Granule size distribution
GSD
High-shear mixer
Growth behaviour
Regime map
Sieving
Agglomeration

ABSTRACT

The aim of this study was to investigate the applicability of the regime map approach proposed by Litster/Iveson and co-workers [S.M. Iveson, J.D. Litster, Growth regime map for liquid-bound granules, AIChE Journal 44 (1998) 1510–1518; S.M. Iveson, P.A.L. Wauters, S. Forrest, J.D. Litster, G.M.H. Meesters, B. Scarlett, Growth regime map for liquid-bound granules: further development and experimental validation, Powder Technology 117 (2001) 83–97] over the whole parameter range, for a given material and agglomeration method. Agglomeration behaviour in a high-shear mixer granulator was investigated and categorised using the evolution of granule size distribution (GSD). MCC 102 (Microcrystalline cellulose, Avicel 102) and aqueous PEG 6k (Polyethylene Glycol 6000) were employed as solid and liquid materials. Different operating conditions were applied by changing impeller speeds and L/S (liquid-to-solid) ratios (weight of liquid/weight of solid). 12 representative settings were selected and typical agglomeration behaviours were identified, forming a regime map for the system. The effect of impeller speed was found to depend on the L/S ratio, very little effect being seen at low L/S ratio (L/S = 85/150), but much more effect at higher binder ratios. In general, the effect of L/S ratio is of paramount importance in these systems and usually determines the growth behaviour.

1. Introduction

Wet agglomeration is a widely applied process in which fine particles are combined to form larger, more easily handled, granules by mixing with a suitable binder. It is a fundamental technique for many industries, particularly pharmaceutical materials handling, mining processes and advanced materials processing, because it can greatly influence the granule properties. For example, in catalysis/absorbents industry, high-shear granulation is used to modify the properties of products (strength, attrition resistance, porosity, and surface area) and thereby to control the efficiency of a chemical reaction [3]. In the pharmaceutical industry, Lee and his co-workers [4,5] have also revealed correlations between drug dissolution rate and the properties of granules (Carr's index, mixing index, surface area, and particle size distribution) in wet granulation. There are, however, many operating variables and these interact with each other, leading to complex behaviour and it is often a challenge to manufacture products consistently to specification [3,6,7]. Therefore a better understanding of granulation mechanisms is required for predicting growth behaviour, as well as to achieve optimal control.

Since 1998, work has been directed to produce regime maps that describe and enable prediction of granule growth in equipment such as rotating drums and high-shear mixers [1,2,8]. These maps show how growth behaviour (changing rate of growth with time) is determined by the work done to deform the granules relative to their deformability (characterized by a *Stokes deformation number* (St_{def})) and the maximum saturation states of granules (characterized by the *maximum pore saturation* (S_{max})). The map from Litster et al. [1,2,8], shown in Fig. 1, identifies four classes of agglomeration growth behaviour: nucleation, steady growth, induction and rapid growth. Nucleation occurs when the binder is brought into contact with a powder bed and granule nuclei are formed, but there is not enough binder to promote further growth. With more binder addition, granules will start to grow and the rate of growth will depend on the deformability of the granules and/or the rate of work done. At the start of granulation, binder tends to get trapped in pockets within granules. The key to growth is redistribution of binder to the surface so that granules can stick together. If the granules are weak or deformable then the process of redistribution is rapid and granules tend to grow immediately and at a steady rate (steady growth). With stronger granules, or less powerful agglomeration processes,

* Corresponding author. Tel.: +886 3 426 7341; fax: +886 3 425 4501.
E-mail address: sshsiau@cc.ncu.edu.tw (S.-S. Hsiau).

1385-8947/$ – see front matter © 2008 Elsevier B.V. All rights reserved.
doi:10.1016/j.cej.2008.09.033

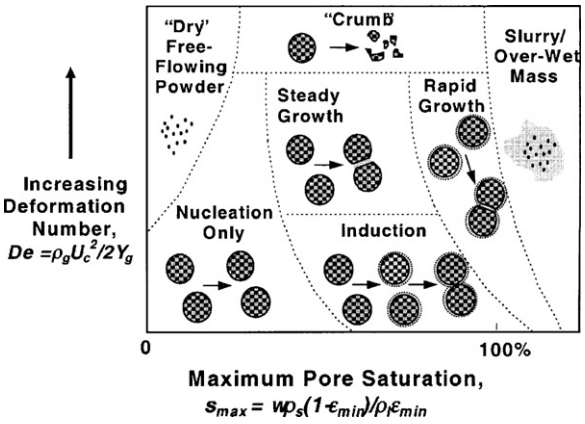

Fig. 1. Granule growth regime map, where ρ_g is the granule density, U_c is the representative collision velocity in the granulator, Y_g is the dynamic yield stress, w is the mass ratio of liquid-to-solid, ε_{min} is the minimum porosity for the particular set of operating conditions and ρ_l is the liquid density [2].

the redistribution process will be slower and the so-called induction behaviour is observed. This is characterised by an initial period of zero overall growth until sufficient binder reaches the granule surface for coalescence and subsequent growth. Eventually, a stable granule size will be achieved [9].

It is noted that the boundaries between these behaviours will depend on the materials, the shear force distribution and heat transfer. Furthermore, because the map defines agglomeration behaviour based on observations of the change of mean granule diameter with time, regardless of other characteristics of the granules, there is an implication that the picture is incomplete. Due to the fast-varying demands from industry, a better understanding of the mechanisms is required. However, information on granule time-dependent characteristics (e.g. surface stickiness, hardness, deformability, shape, granule size distribution, force distribution and particle friction forces) is still sparse.

Modern theories of agglomeration incorporating a series of stages have been developed recently [9–14]. These theories describe the agglomeration process as a combination of three major mechanisms: (1) wetting and nucleation, (2) consolidation and aggregation and (3) breakage and attrition. Although these stages are usually considered as sequential, growth and breakage of granules are expected to occur simultaneously owing to the inhomogeneous shear force distribution inside the working vessel [9,15]. Bouwman et al. [16] experimentally validated this concept by revealing that solid material exchange indeed took place during the equilibrium stage in high-shear mixers. In order to treat distributions of particle size, a population balance must be applied [13,17–23]. The general equations of this type of theory are able to incorporate aggregation (volume coalescence) of particles from the same or different size classes, and breakage, although general expressions for fragmentation are difficult to determine. Rates of increase of the fraction of discrete size classes (birth) are described by nucleation, growth and agglomeration kernels while rates of decrease (death) are described by agglomeration and breakage kernels [22,24].

This paper demonstrates the general effects of impeller speed and liquid/solid (L/S) ratio over a wider range than is usual, in order to obtain a regime map, with particular attention paid to the change of granule size distribution (GSD) during the granulation process. The importance of GSD for understanding agglomeration processes has been emphasized [9], because it can provide additional quantitative observations for the underlying mechanisms, which mean granule size may conceal.

2. Experiment

2.1. Materials

MCC Avicel 102 (Microcrystalline Cellulose, Avicel 102, d_{50} = 125.3 μm) was used as the solid material. It exhibits the physical properties of being inert and odourless, and unique agglomeration characteristics; hence it is commonly used in the pharmaceutical industries, especially for tableting, formation of granules and capsules. The chosen binder material was a 33% aqueous solution of PEG 6k (Polyethylene Glycol 6000), with a viscosity of 0.0324 Pa s at 25 °C. Different amounts of binder were mixed with a fixed amount of powder and the mix was granulated under a certain range of impeller speeds, representing different saturation states and particle collision speeds in the system.

2.2. Experimental setups and processes

The specially constructed lab-scale high-shear mixer, shown in Fig. 2 that been used in many previous studies [25,26] was employed again in this research. The stainless steel working vessel was 13.3 cm in inner diameter and 20.5 cm in depth. A replaceable three-bladed impeller made of mild steel was centrally located on the base of the vessel. Each blade on the impeller is identical and has the leading edge inclined by 13°. The rotational speed of the impeller is electronically controlled and can be adjusted from 0 to 3000 rpm.

There are two effects that should be noted when comparing this mixer with those in industry: (1) the absence of a chopper and (2) the effects of scale. According to the literature, the effects of a chopper are mainly determined by the size and shape of the blades

Table 1
Experimental setups employed in this study.

No.	Impeller speed (rpm)	L/S ratio (w/w)	Flow rate of binder addition (g/s)	Sampling times
1	600	85/150	2.833	10
2	450	85/150	2.833	10
3	300	85/150	2.833	10
4	600	110/150	3.667	10
5	450	110/150	3.667	10
6	300	110/150	3.667	10
7	600	130/150	4.333	10
8	450	130/150	4.333	10
9	300	130/150	4.333	11
10	600	150/150	5.000	10
11	450	150/150	5.000	10
12	300	150/150	5.000	10

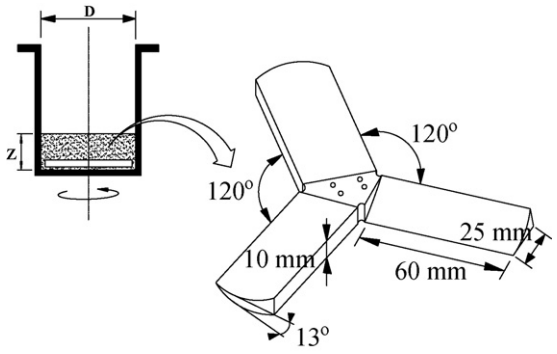

Fig. 2. Schematic drawing of the high-shear mixer and the three-bladed impeller.

[11,27,28]. Short blunt blades tend to densify the granules while longer sharper ones will break up the lumps. Another difference is the scale. Comparing to a larger scale, the intra-granular structure (porosity) is looser in a smaller scale due to slower peripheral velocity and minor centrifugal effects.

A plastic scoop was used as a granule-sampling device throughout experiments. The sampling time was defined as the average of an interval, e.g., any sample taken from 55 to 65 s was considered as from the 60th second. In order to obey the golden rules for powder sampling [29], sampling was made from two fixed and symmetric locations in the powder bed while the experiments were running. One sample comprised two identical sized extractions, one from each location within 5 s of each other. The sampling locations in this paper were set at the middle point between the centre and the tip of the impeller, and the middle height of the powder bed.

150 g of MCC was required in each experiment to fill the mixer in a ratio of $Z/D = 0.26$ [30], where Z is the height of the stationary dry powder bed and D represents the inner diameter of the mixer shown as Fig. 2. In order to minimize any possible inconsistencies in the state of the bed following loading, it was "stirred" with the impeller at 100 rpm for 30 s before the binder was added. The binder was then added to the mixer by pouring at the middle point between the centre and the tip of the impeller, the addition being completed within 30 s. The fill time was the same regardless of the amount of binder added. The binder addition rate and formulae of solid and liquid are listed in Table 1 and shown in Fig. 3 as a working matrix. A stopwatch was started immediately after complete addition of the binder. For size characterization, granule samples were then carefully removed from the mixer using the plastic sampling scoop at prescribed intervals, and immediately spread onto a tray for cooling at room temperature.

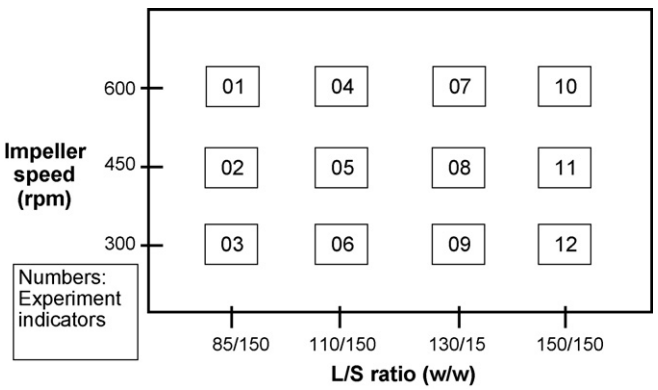

Fig. 3. Working matrix of experimental setup.

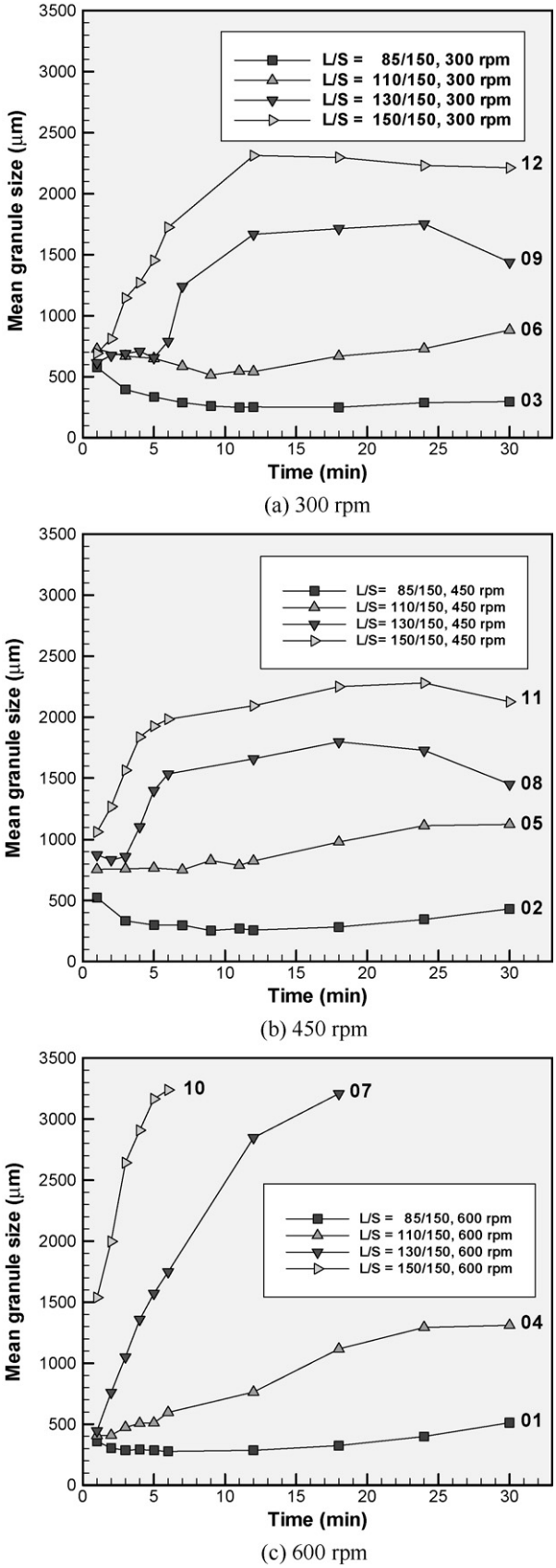

Fig. 4. Comparisons under the same impeller speeds.

According to Table 1, at least 10 repeated samplings were to be made from a confined mixer. Therefore it was necessary to minimise the size of each sample to avoid a change in conditions as the experiment progressed. In order to give statistically significant results, each experiment was performed three times and the GSD obtained was the average from three experiments. The total amount of material removed by sampling in each single experiment was always less than 10% of the total weight of the mixture.

In this paper, considering the wide spread in GSD, the particle sizing was carried out following standard sieving procedures, because sieving, compared to optical techniques such as diffraction, is a reliable and reproducible technique for measuring wide size distributions, e.g. 30–4000 μm. Size distributions were obtained using the assumption that mean granule size on each sieve equalled the arithmetic mean value of the collecting sieve and the one above it. To minimize the breakage of granules and agglomeration on the mesh, the samples were left in an oven and dried overnight at 40 °C before sieving, so that the granules were robust and would not be affected by surface stickiness. Tests have been done and shown that GSD does not change with repeated sieving.

3. Results and discussion

3.1. Effects of the L/S ratio and impeller speed

Fig. 4 shows the effects of varying the amount of binder addition on granule growth behaviour at impeller speeds of 300, 450 and 600 rpm, respectively. It can be seen that granule growth rate and the final mean granule size were profoundly determined by the amount of liquid added. High L/S ratio led to rapid growth and large granule sizes, particularly at high-impeller speed.

The effects of the impeller speed are shown in Fig. 5. It can be seen that the agglomeration behaviour at low L/S ratios (L/S = 85/150, 110/150) was largely unaffected by the impeller speed. At higher level of saturation (L/S = 130/150 and 150/150), there was an effect of impeller speed. Between 300 and 450 rpm, the effect was small, but above 450 rpm, there was a significant increase on the rate of granule growth and the ultimate size achieved. Therefore, binder addition is the primary determinant of granulation behaviour because it is only at higher L/S ratio that behaviour is sensitive to changes in impeller speed. If saturation is kept low,

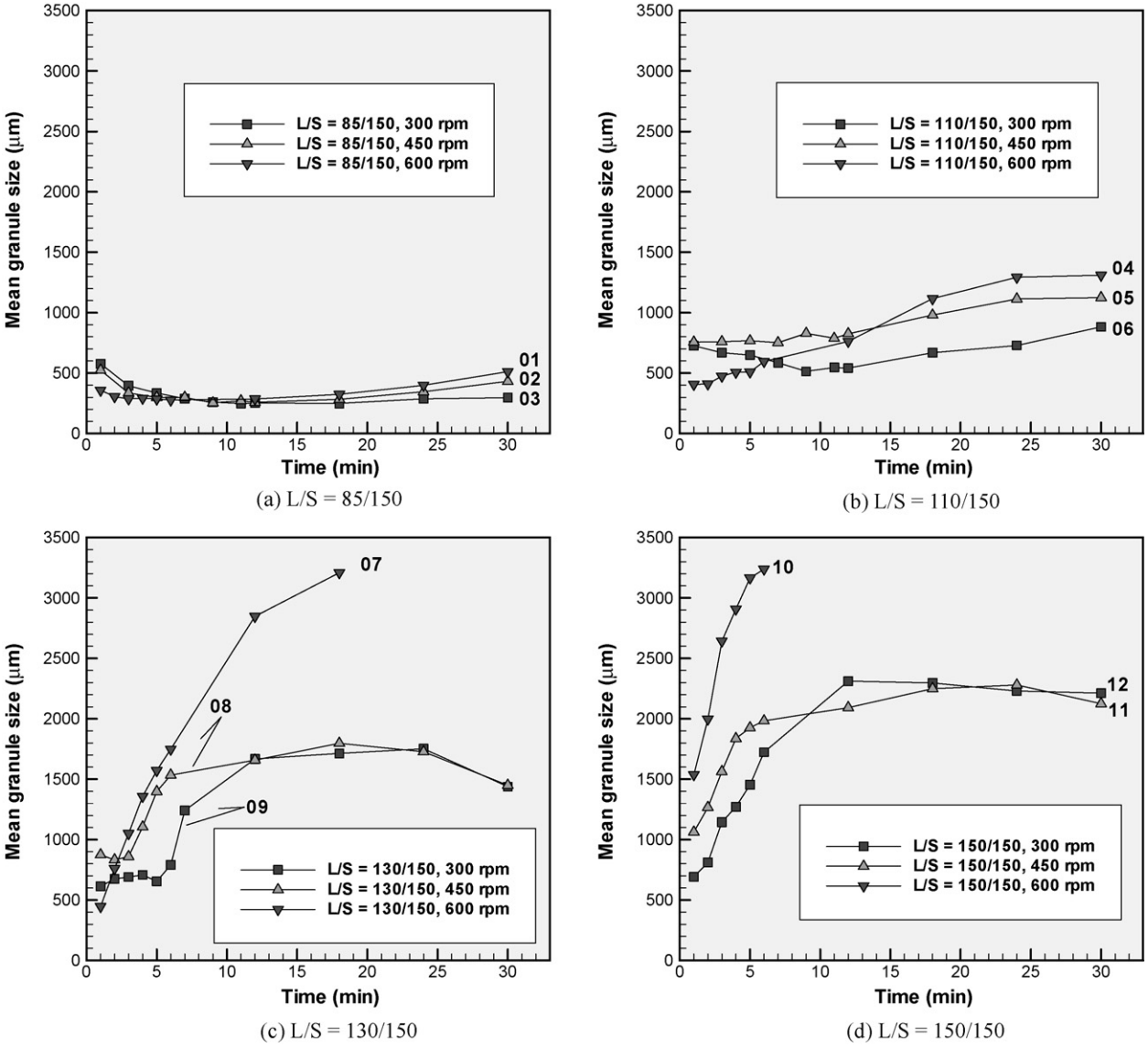

Fig. 5. Comparisons under the same L/S ratios.

growth is limited and increasing impeller speed does not compensate for the lack of binder. It is clear that the key to granulation is sufficient binder but not excess otherwise growth can go out of control. With adequate binder present, the growth rate and final mean size can be controlled by the impeller speed, but the effect is not linear. This may imply that the deformability of the granules is non-linear, perhaps following a Herschel–Bulkley or power law type rheological model.

3.2. GSD and the change of specific granules sizes

Figs. 6–10 represent the evolution of size distribution from the change of mass fraction of each specific granule size obtained from sieving. The size distributions have been normalised by dividing the abscissa by log aperture. In order to follow changes with time more easily, the size distributions have been separated into four groups with respect to size: 0–550 μm (or 0–605 μm), 550–1200 μm (or 605–1200 μm), 1200–2400 μm and 2400–3400 μm, respectively. The total weight in each group was summed up and plotted against time, in order to correlate the change in mean granule size with the changes in each mass fraction.

3.2.1. Nucleation only

Fig. 6(a) shows how the GSD for experiment 03 changes with time. Almost identical GSDs were observed for experiments 01 and 02 hence it was concluded that these low binder content (L/S = 85/150) experiments displayed the same growth behaviour. The relatively large mean granule size at the start of these runs (see Fig. 5(a)) are attributable to slow-to-disperse big clumps being formed by uneven binder distribution following addition, indicated by the circle in Fig. 6(a).

Fig. 6(b) tracks the change of mass fractions of the four size classes selected. This shows a small increase in the fines (0–550 μm) fraction initially, at the expense of a slight decrease in the larger size classes, particularly the largest, indicating some break-up. A little agglomeration occurred thereafter (into intermediate size fractions) but due to the lack of binder, granules were unable to agglomerate effectively and the mean granule size was nearly independent of time. Clearly then, there is little happening here apart from the binder being distributed among very small granules or nuclei. Hence for L/S = 85/150 the behaviour was classified as nucleation only.

3.2.2. Steady growth

When L/S ratio was increased to 110/150, the mean granule size increased steadily but slowly with time as seen in Fig. 5(b); therefore the granulation process under these conditions was classified as steady growth behaviour. Furthermore, the peak of the GSD for experiment 04 (shown in Fig. 7(a) and chosen as representative for this mode of behaviour) shows a steady monotonic increase as granulation proceeds. There is a suggestion that agglomeration becomes unstable between 24 and 30 min, as the final GSD is less smooth and shows an increase in the fraction of large granules. This has not been investigated further. As with the nucleation mode experiments, there are some large granules present initially. Fig. 7(b)–(d) shows the change in mass fractions of four size classes: 0–605, 605–1200, 1200–2400, 2400–3400 μm. At low speed (Fig. 7(b)), there is a steady decrease in fines accompanied by a steady increase in the fractions of the larger classes. It is seen that the onset of growth of the larger classes tends to lag behind that of the class below, implying a layering mechanism, particularly with the lowest impeller speed. With increasing impeller speed we see an interesting phenomenon: rapid initial growth of the 605–1200 μm particles followed by decline and subsequent increase. This is mirrored by equal but opposite changes in the mass fraction of the 0–605 μm particles. This might imply that the early granules formed are weak and short lived but as the distribution of the binder improves and the granules become more consolidated they become stronger and less prone to breakage.

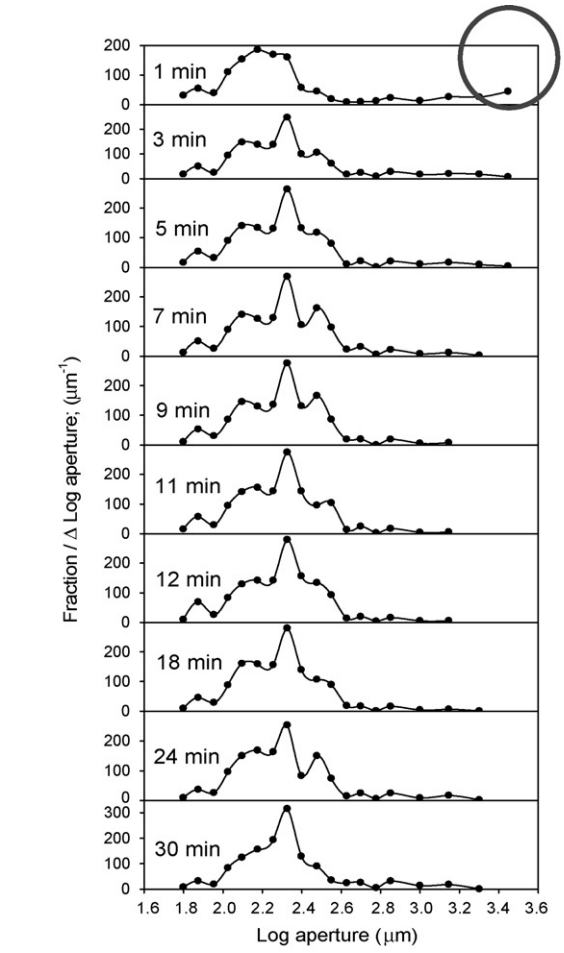

(a) The GSD of experiment 03

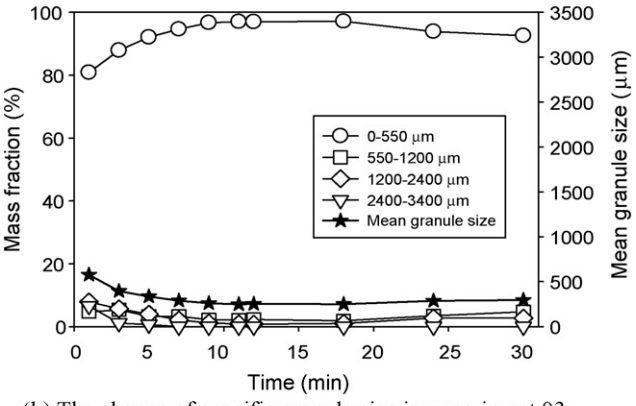

(b) The change of specific granule size in experiment 03

Fig. 6. GSD and the change of specific granule size in the behaviour of nucleation only (experiment 03).

In summary, for the combination of conditions in this group, the growth process is a competition between growth and breakage. Overall, granule growth was faster at higher speeds and led to larger granules than at lower speeds.

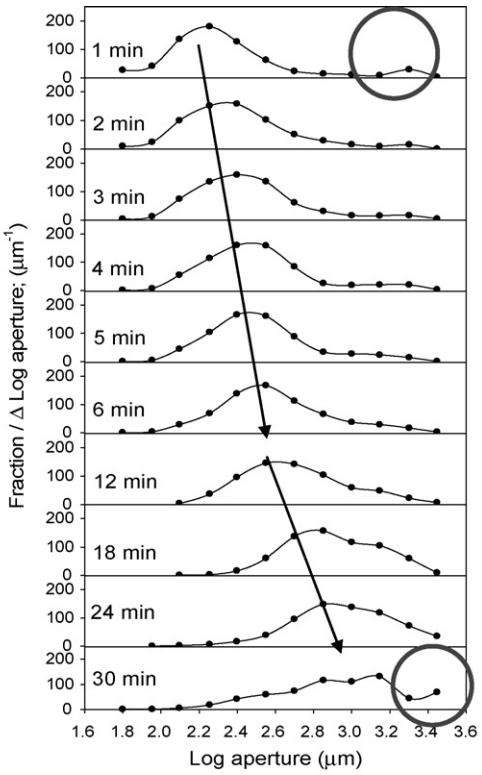

(a) The GSD of experiment 04

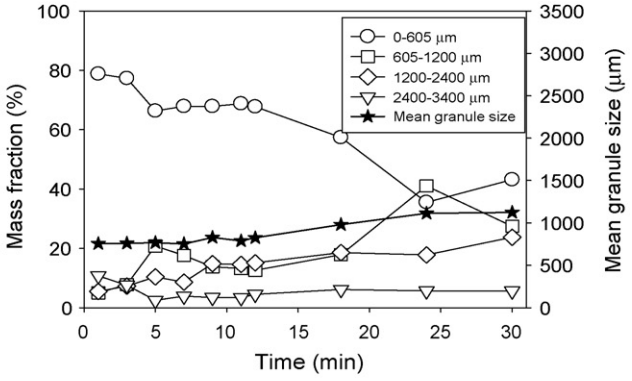

(c) The change of specific granule size in experiment 05

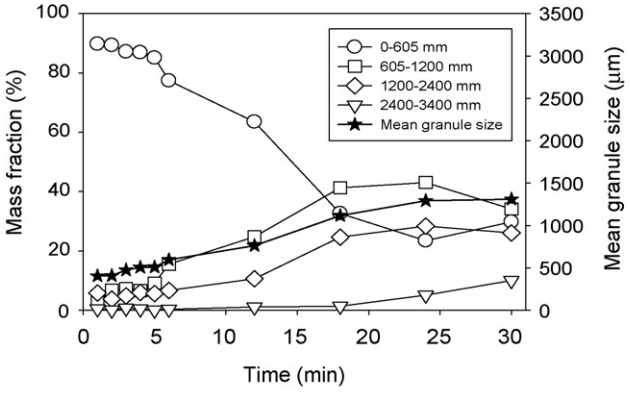

(b) The change of specific granule size in experiment 04

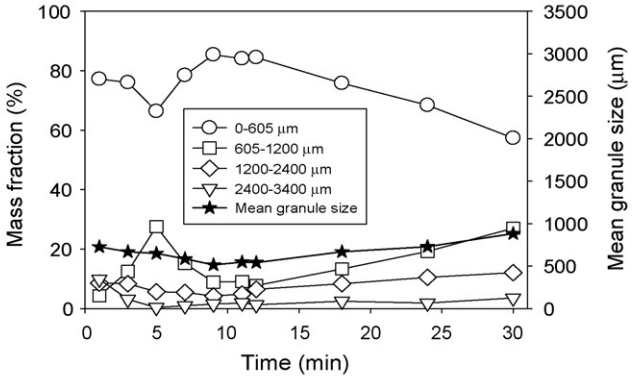

(d) The change of specific granule size in experiment 06

Fig. 7. GSD and the change of specific granule size in the behaviour of steady growth (experiments 04, 05 and 06).

3.2.3. Induction behaviour

Experiments 08 and 09 displayed typical characteristics of induction behaviour:

(1) *Induction stage*: As observed in Fig. 5(c), the mean granule size remains relatively constant for a period in the early stages due to the compensating effects of simultaneous growth and destruction of large clumps. These competing mechanisms can be seen clearly in Fig. 8(a) and (b) where both the fractions of clumps and fines are decreasing at this stage.

(2) *Rapid growth stage*: after a period, while the decrease of clumps and fines proceeds, the mean granule size increases suddenly and rapidly, indicating that a more uniform binder distribution among granules might be required for the start of this second stage.

(3) *Equilibrium stage*: after the rapid growth, a plateau in mean size appears. This is presumably a result of equilibrium between breakage and growth. No further binder can be squeezed to the surface, so granules are unable to coalesce further. However, this stage is not always stable and in the two cases shown, a perturbation of each size fraction results at long times. The equilibrium mean granule size observed in experiments 08 and 09 (450 and 300 rpm, respectively) were found to be very similar, in spite of the different induction periods, indicating that induction type behaviour leads to the same endpoint for a given binder content even with different rates of the mechanisms.

By tracking the change in mass fraction of specific granule size classes as shown in Fig. 8(a) and (b), the mechanisms of this behaviour can be seen more clearly: during the induction and rapid

growth stages, the mass fraction of each specific size class varied with time. An increase of bigger granules was accompanied by a decrease of smaller ones. This corresponds to the idea of the consolidation-layering mechanism [31] which proposes that, during the induction stage, fine powders will be layered onto the bigger granules (decrease of fines) as granule consolidation squeezes liquid to the surface. Following layering, these larger "layered" granules coalesce with each other as shown by the rapid increase in mass fraction of bigger granules. Interestingly, a similar exchange process was observed here for all the operating conditions, but only certain conditions display this induction behaviour. It is still unclear whether the exchange of material is necessary for this behaviour. It seems that inter-granular material exchange is not sufficient to explain the induction behaviour. Exchange of material must be critical for growth because this is one of the methods that binder gets distributed and this is true for all mechanisms. However, it is still unclear whether the time for induction is to achieve distribution of binder among the granules or within the granules, i.e. consolidation.

It is important to remember that while a changing size fraction will imply material exchange, the converse does not necessarily follow: in the equilibrium stage, mass fractions of the classes remain constant but material exchange has been shown to still occur [16].

The effect of increasing the impeller speed in this behavioural regime was to shorten the induction time without affecting the final mean granule size. Further increase in speed to 600 rpm eliminated the induction period: the agglomeration went straight into unconstrained growth in which the granules became too big to be measured within a few minutes (see Section 3.2.5).

3.2.4. Rapid growth

Fig. 5(d) shows agglomeration behaviour for the highest L/S ratio (150/150). The mean granule sizes for experiments 11 and 12 increased immediately on binder addition and exhibited typical rapid growth characteristics. Referring to the mass fractions of each specific size (Fig. 9(a) and (b)), it can be seen that small granules disappeared within the first few minutes while in the same time frame, the fraction of larger granules increased to a plateau. This indicates that, initially, growth significantly overwhelms breakage but equilibrium is soon reached with growth and breakage in balance. It is shown later (Section 3.2.5) that higher impeller speeds cause rapid consolidation of the granules, leading to a higher saturation state and growth continues to be dominant: no steady state is reached. The rate of growth in the rapid growth period increased with increasing impeller speed.

It is interesting that experiment 07, with less binder than experiment 12, leads to uncontrolled growth (see the following section) while experiment 12 reaches a steady state. It might be expected that the conditions of lower binder and higher impeller speed would lead to smaller granules for number 07. Clearly it is not just the binder content that matters but the distribution of this binder caused by the impeller. This is probably related to intra-granular binder distribution (consolidation).

These findings are consistent with the growth regime map [1,2], which suggests that high-impeller speed leads to crumb formation with little binder in the system but rapid growth when more binder is added.

3.2.5. Unconstrained growth

When the critical amount of binder addition L/S = 130/150 was reached, the highest impeller speed 600 rpm resulted in the growth behaviour going out of control. The mean granule sizes of experiments 07 and 10 were increased dramatically and therefore exceeded the sieving resolution in a short time. Thus the behaviour was categorised as unconstrained growth. As in the earlier examples of rapid growth, Fig. 10(a) and (b) shows that increase of mass in the larger classes corresponds to decrease of mass in the smaller ones. It has been commented earlier that the conditions for this type of growth must be a combination of absolute binder content and binder distribution within the granules.

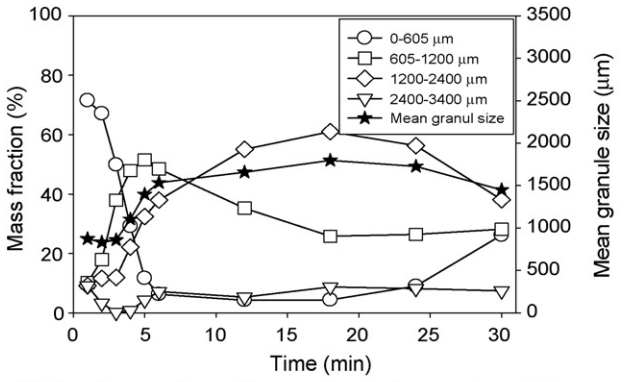

(a) The change of specific granule size in experiment 08

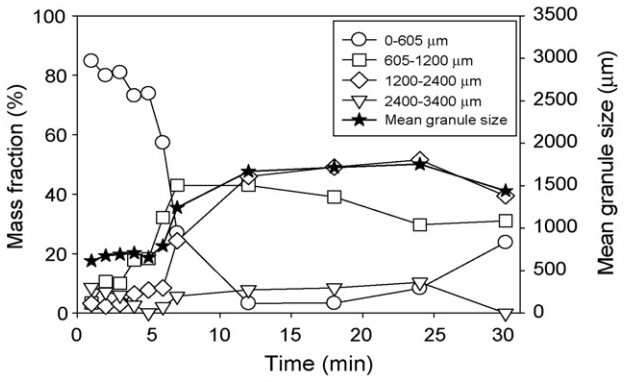

(b) The change of specific granule size in experiment 09

Fig. 8. The change of specific granule size in the behaviour of induction growth (experiments 08 and 09).

3.3. Regime map for the system

The experiments were performed by following the working matrix given in Fig. 3 and Table 1 and characterised with the analysis of GSD and the change in mass fraction of specific granule size classes. Five growth behaviours, i.e. nucleation, steady growth, induction behaviour, rapid growth and unconstrained growth were identified. Boundaries have been drawn to separate the growth behaviour in terms of the L/S ratio and impeller speed to create a regime map shown in Fig. 11. Impeller speed is plotted on the ordinate axis, and L/S ratio is plotted on the abscissa.

Traditionally, the dynamic yield stress Y_g in the regime map (Fig. 1) is measured on systems in which the powder and binder are well mixed [13]. Furthermore, the abscissa, S_{max} implies that all granules are at the maximum saturated state and obscures the fact that, in the early stages at least, there is a wide range of saturation with material anywhere between the two extreme cases: over-wetted and dry-flowing.

This paper has developed a specific map in terms of the operating condition (impeller speed instead of deformation number and L/S instead of S_{max}), simply because this is more practical and more meaningful given the heterogeneous and time dependent nature of granulation. There has also been an attempt to understand the agglomeration process by viewing the evolution of the granule size distribution alongside the rate of granulation. It is clear that time is

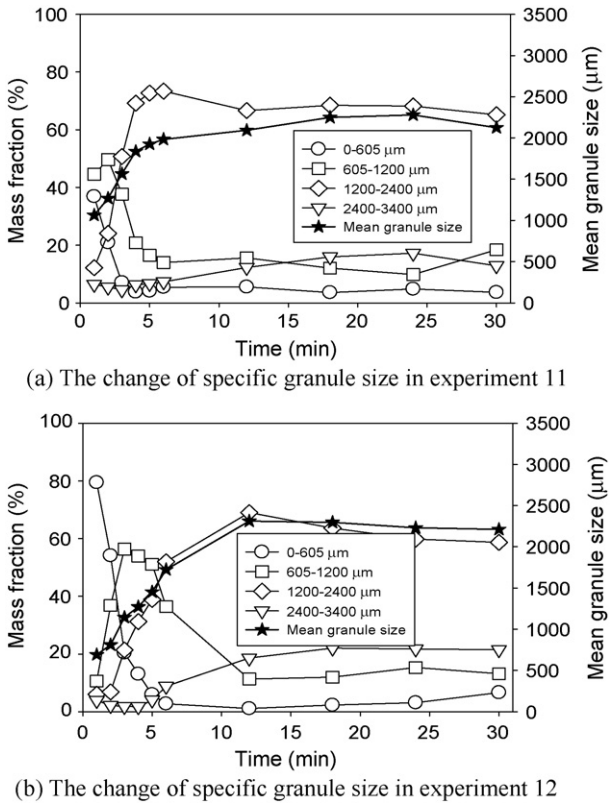

(a) The change of specific granule size in experiment 11

(b) The change of specific granule size in experiment 12

Fig. 9. The change of specific granule size in the behaviour of rapid growth (experiments 11 and 12).

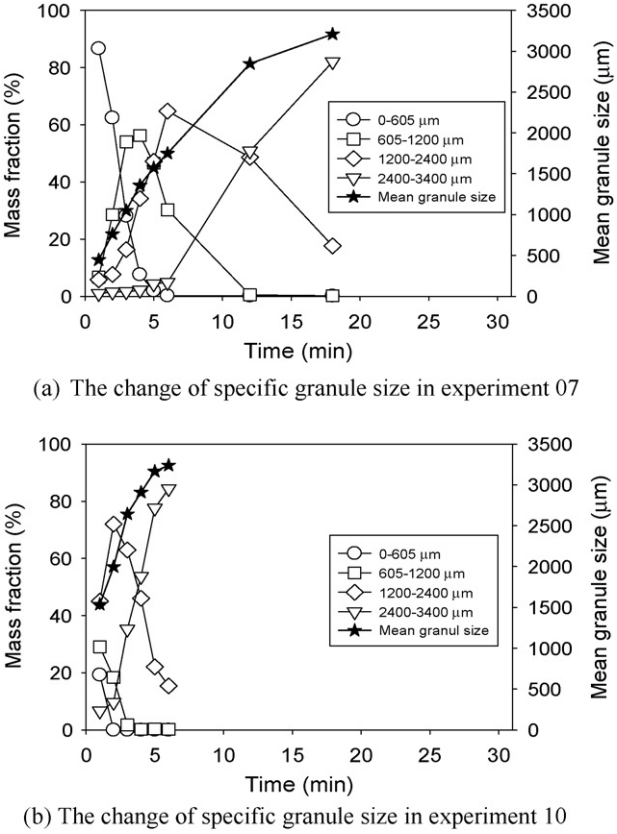

(a) The change of specific granule size in experiment 07

(b) The change of specific granule size in experiment 10

Fig. 10. The change of specific granule size in the behaviour of unconstrained growth (experiments 07 and 10).

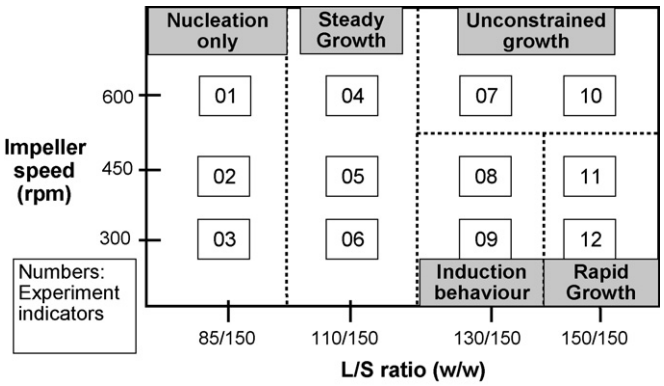

Fig. 11. The regime map for the system.

an important third dimension in these maps, not just because this is a growth process but also because there is significant material exchange occurring between and within granules.

Rough et al. [32] have also attempted to consider the time effect by superimposing the granulation processes on the map, however they did not investigate the relations between material exchange (GSD) and behaviour. Also, they did not measure the Y_g satisfactorily. In practice, measuring Y_g convincingly is still difficult until the GSD and binder distribution become steady. Furthermore, like granule size, Y_g may be a distributed property, particularly in the early stages when binder distribution is inhomogeneous. It is not clear whether uniform binder distribution necessarily leads to uniform Y_g regardless of GSD. This uncertainty is worthy of further investigation.

4. Conclusions

The present research demonstrates the overall effects of impeller speed and L/S ratio on granulation behaviour. The effect of impeller speed is dependent on the L/S ratio. It has a trivial effect on the mean granule size when little binder is added but a significant effect with more binder in the system: increasing speeds leads to increased rate of granule growth and ultimately larger particles. This shows that while sufficient binder is a requirement for granule growth there is an equally important requirement for distribution of this binder and that low impeller speeds impart insufficient energy to achieve this.

This work also demonstrates the utility of the regime map proposed by Litster/Iveson and co-workers. This has shown that a single system of solid and binder can exhibit five distinctly different growth patterns, as observed from measurement of changes in GSD and the mass fractions of discrete granule size classes with time. Both examinations showed that birth and death of granules took place simultaneously during certain stages, as set out in the general concept of population balance models. In some regimes, growth behaviour is extremely sensitive to operating conditions. It is also the case that the same type of growth behaviour can be lead to subtly different GSD.

Acknowledgements

The authors would like to express their gratitude to the financial supports granted by the Graduate Student Study Abroad Program, and NSC 97-2628-E-008-036-MY3 from National Science Council, Taiwan, R.O.C., and to the Department of Chemical Engineering, University of Birmingham, for use of equipment and additional financial supports to the first author. They also thank Mr. Kel Win Chua from Particle Products Group, University of Sheffield for dis-

cussion of population balance equations, and Professor Tu Lee from Chemical & Materials Engineering, National Central University Taiwan, for providing his insight into this research.

References

[1] S.M. Iveson, J.D. Litster, Growth regime map for liquid-bound granules, AIChE Journal 44 (1998) 1510–1518.
[2] S.M. Iveson, P.A.L. Wauters, S. Forrest, J.D. Litster, G.M.H. Meesters, B. Scarlett, Growth regime map for liquid-bound granules: further development and experimental validation, Powder Technology 117 (2001) 83–97.
[3] E.M. Holt, The properties and forming of catalysts and absorbents by granulation, Powder Technology 140 (2004) 194–202.
[4] T. Lee, H.J. Hou, H.Y. Hsieh, Y.C. Su, Y.W. Wang, F.B. Hsu, The prediction of the dissolution rate constant by mixing rules: the study of acetaminophen batches, Drug Development and Industrial Pharmacy 34 (2008) 522–535.
[5] T. Lee, F.B. Hsu, A cross-performance relationship between Carr's index and dissolution rate constant: the study of acetaminophen batches, Drug Development and Industrial Pharmacy 33 (2007) 1273–1284.
[6] F.J. Muzzio, T. Shinbrot, B.J. Glasser, Powder technology in the pharmaceutical industry: the need to catch up fast, Powder Technology 124 (2002) 1–7.
[7] H. Leuenberger, M. Lanz, Pharmaceutical powder technology—from art to science: the challenge of the FDA's Process Analytical Technology initiative, Advanced Powder Technology 16 (2005) 3–25.
[8] S.L. Rough, D.I. Wilson, A.E. Bayly, D.W. York, Mechanisms in high-viscosity immersion-granulation, Chemical Engineering Science 60 (2005) 3777–3793.
[9] S.M. Iveson, J.D. Litster, K. Hapgood, B.J. Ennis, Nucleation, growth and breakage phenomena in agitated wet granulation processes: a review, Powder Technology 117 (2001) 3–39.
[10] P. Vonk, C.P.F. Guillaume, J.S. Ramaker, H. Vromans, N.W.F. Kossen, Growth mechanisms of high-shear pelletisation, International Journal of Pharmaceutics 157 (1997) 93–102.
[11] F. Hoornaert, P.A.L. Wauters, G.M.H. Meesters, S.E. Pratsinis, B. Scarlett, Agglomeration behaviour of powders in a Lodige mixer granulator, Powder Technology 96 (1998) 116–128.
[12] A. Goldszal, J. Bousquet, Wet agglomeration of powders: from physics toward process optimization, Powder Technology 117 (2001) 221–231.
[13] S.M. Iveson, J.A. Beathe, N.W. Page, The dynamic strength of partially saturated powder compacts: the effect of liquid properties, Powder Technology 127 (2002) 149–161.
[14] K.P. Hapgood, J.D. Litster, S.R. Biggs, T. Howes, Drop penetration into porous powder beds, Journal of Colloid and Interface Science 253 (2002) 353–366.
[15] W.J. Wildeboer, J.D. Litster, I.T. Cameron, Modelling nucleation in wet granulation, Chemical Engineering Science 60 (2005) 3751–3761.
[16] A.M. Bouwman, M.R. Visser, G.M.H. Meesters, H.W. Frijlink, The use of Stokes deformation number as a predictive tool for material exchange behaviour of granules in the 'equilibrium phase' in high shear granulation, International Journal of Pharmaceutics 318 (2006) 78–85.
[17] M.J. Hounslow, J.M.K. Pearson, T. Instone, Tracer studies of high-shear granulation. II. Population balance modeling, AIChE Journal 47 (2001) 1984–1999.
[18] S.M. Iveson, Limitations of one-dimensional population balance models of wet granulation processes, Powder Technology 124 (2002) 219–229.
[19] X. Liu, D. Litster, Population balance modelling of granulation with a physically based coalescence kernel, Chemical Engineering Science 57 (2002) 2183–2191.
[20] D. Verkoeijen, G.A. Pouw, G.M.H. Meesters, B. Scarlett, Population balances for particulate processes—a volume approach, Chemical Engineering Science 57 (2002) 2287–2303.
[21] P.A.L. Wauters, B. Scarlett, L.X. Liu, J.D. Litster, G.M.H. Meesters, A population balance model for high shear granulation, Chemical Engineering Communications 190 (2003) 1309–1334.
[22] A. Darelius, A. Rasmuson, I.N. Björn, S. Folestad, High shear wet granulation modelling—a mechanistic approach using population balances, Powder Technology 160 (2005) 209–218.
[23] A. Darelius, H. Brage, A. Rasmuson, I.N. Björn, S. Folestad, A volume-based multi-dimensional population balance approach for modelling high shear granulation, Chemical Engineering Science 61 (2006) 2482–2493.
[24] J.M.H. Poon, C.D. Immanuel, F.J.I. Doyle, J.D. Litster, A three-dimensional population balance model of granulation with a mechanistic representation of the nucleation and aggregation phenomena, Chemical Engineering Science 63 (2008) 1315–1329.
[25] P.C. Knight, J.P.K. Seville, A.B. Wellm, T. Instone, Prediction of impeller torque in high shear powder mixers, Chemical Engineering Science 56 (2001) 4457–4471.
[26] R.H. Bridson, P.T. Robbins, Y. Chen, D. Westerman, C.R. Gillham, T.C. Roche, J.P.K. Seville, The effects of high shear blending on alpha-lactose monohydrate, International Journal of Pharmaceutics 339 (2007) 84–90.
[27] K. Saleh, L. Vialatte, P. Guigon, Wet granulation in a batch high shear mixer, Chemical Engineering Science 60 (2005) 3763–3775.
[28] P.C. Knight, An investigation of the kinetics of granulation using a high shear mixer, Powder Technology 77 (1993) 159–169.
[29] T. Allen, Particle Size Measurement, Powder Sampling and Particle Size Measurement, Chapman & Hall, 1997.
[30] G.I. Tardos, K.P. Hapgood, O.O. Ipadeola, J.N. Michaels, Stress measurements in high-shear granulators using calibrated "test" particles: application to scale-up, Powder Technology 140 (2004) 217–227.
[31] K.P. Hapgood, S.M. Iveson, J.D. Litster, L.X. Liu, Granulation rate processes, in: A.D. Salman, M.J. Hounslow, J.P.K. Seville (Eds.), Granulation, Elsevier, Amsterdam, 2007, pp. 897–978.
[32] S.L. Rough, D.I. Wilson, D.W. York, A regime map for stages in high shear mixer agglomeration using ultra-high viscosity binders, Advanced Powder Technology 16 (2005) 373–386.